Macromolecules

ARTICLE

pubs.acs.org/Macromolecules

# Segmental Relaxation of Hydrophilic Poly(vinylpyrrolidone) in Chloroform Studied by Broadband Dielectric Spectroscopy

Naoki Shinyashiki,*[,†] Anna Spanoudaki,[‡] Wataru Yamamoto,[†] Eri Nambu,[†] Kaoru Yoneda,[†] Apostolos Kyritsis,[‡] Polycarpos Pissis,[‡] Rio Kita,[†] and Shin Yagihara[†]

[†]Department of Physics, Tokai University, Hiratsuka, Kanagawa 259-1292, Japan

[‡]Department of Applied Mathematics and Physics, National Technical University of Athens, Heroon Polytechneiou 9, 15780 Athens, Greece

**ABSTRACT:** Dielectric relaxation caused by the segmental motion of poly(vinylpyrrolidone) (PVP) was studied in chloroform solutions with 5−40 wt % PVP at temperatures between 298 and 210 K above the melting temperature of chloroform (210 K) to obtain information on the dynamics of hydrophilic polymer. The asymmetric broadening of the loss peak and the fragility, i.e., the degree of deviation from the Arrhenius temperature dependence of relaxation time, increase with increasing PVP concentration. Both are due to increase in cooperativity of the segmental motion of PVP. The temperature-independent shape of the loss peak at a fixed concentration satisfies the time−temperature superposition and can be interpreted to be due to the small concentration fluctuation in the PVP/chloroform solutions. The repulsive force between PVP chains is expected to make the mixture homogeneous in chloroform, which is a good solvent of PVP.

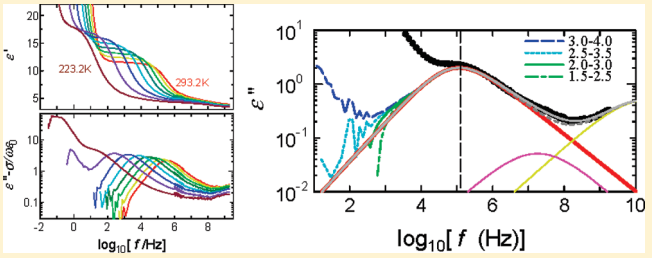


## INTRODUCTION

Despite the fact that the dielectric relaxation process of polymers in a nonpolar solvent has been studied extensively, a few results have been reported on observation of the dynamics of polymers in solutions with a polar solvent in a solvent-rich region.[1−6] The difficulty of observation is caused by the existence of the large contributions of conductivity and electrode polarization to complex dielectric permittivity. Even if the local chain motion of a polymer exists at frequencies lower than those of the polar solvent, the dc conductivity and electrode polarization mask the relaxation process of the chain motion. In this case, the local chain motion of polymers has been detected with a large error[2,4] or has not been detected at all.[7−9] In addition, observation of the dielectric relaxation processes of both solvent and solute polymers requires an extremely wide frequency range. Therefore, the systematic experimental study of the dynamics of a polymer chain in a polar solvent has only recently started.[5,6]

Poly(vinylpyrrolidone) (PVP) is a semicrystalline synthetic polymer that forms a randomly coiled and highly flexible chain in polar solvents. PVP is nontoxic and possesses good biocompatibility and thus has been used in cosmetics, drug delivery systems (DDSs), artificial organs, and so forth. It is known that some polymers exhibit good performance as functional materials in a water−polymer interface, but the mechanisms of the function have not been known yet. It is expected that the function is related to the dynamics of the polymer in aqueous systems. Molecular interactions between PVP and solvent molecules change the dynamics of neat PVP and solvent.

The structure of a repeat unit of PVP is shown in Figure 1a. The repeat unit of PVP has a permanent dipole moment whose magnitude is 3.53 D obtained by ChemOffice Ultra 2004 (CambridgeSoft). The angle between the dipole moment and the bond between carbon at main chain and nitrogen at side group, which is perpendicular to the chain contour, is 78°; i.e., the dipole moment directs almost from O to C of the carbonyl group as shown in Figure 1b. The magnitude of a component of the dipole moment fixed perpendicular to main chain contour (main chain contour is placed parallel to $Z$ axis) corresponds to the type B dipole component[10] is 0.73 D, which fluctuates with micro-Brownian motion of main chain directly related to the glass transition phenomena of PVP. Another component, whose magnitude is 3.45 D, is perpendicular to the type B component of the dipole moment. This component is on the pendant side group connected with main chain through one covalent bond between nitrogen and carbon permitting internal rotation (type C dipole component[10]) . The rotational motion of bulky pendant side group of PVP seems to be interfered with neighboring groups. If it is true, the dipole moments behave as type B. Therefore, the dielectric relaxation of PVP is caused by the rotational motions of type B and C dipole components.

Dielectric studies of PVP solutions have provided a range of important information on molecular dynamics, the degree of intermolecular interaction, and cooperativity between guest and

**Received:** October 21, 2010
**Revised:** February 19, 2011
**Published:** March 11, 2011

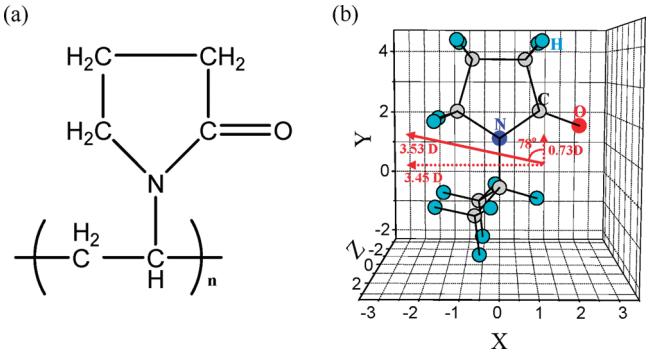


**Figure 1.** (a) Chemical structure of a repeat unit of PVP. (b) Schematic figure of the relationship between the direction of permanent dipole moment of PVP and positions of atoms (Å) determined by ChemOffice Ultra 2004 (CambridgeSoft). The conformation with minimum energy is shown. The main chain contour is placed parallel to the $Z$ axis. The bond between carbon at main chain and nitrogen at the pendant side group is placed parallel to the $Y$ axis. The carbons, nitrogen, and oxygen atoms in the pendant side group are at the single $X-Y$ plane.

host molecules. Furthermore, the dielectric properties of PVP in solution depend on the nature of the solvent. The dielectric behavior of PVP solutions in water,[2,4,5,8,11−20] alcohol,[5,21] and ethylene glycol oligomer (EGO)[1,3] has been extensively studied. We made broadband dielectric measurements of PVP−monohydroxyl alcohol mixtures of various normal alcohols with the number of carbon atoms per molecule ranging from 1 to 9 in the frequency range of 20 Hz−20 GHz at 25 °C.[5] Two relaxation processes due to the reorientation of dipoles on PVP and alcohol molecules were observed. The relaxation process at frequencies higher than 100 MHz is the primary process of alcohols, and that at frequencies lower than 10 MHz is attributed to the local chain motion of PVP. The relaxation time of the local chain motion of PVP increases with PVP concentration and solvent viscosity. Different time scales of the molecular motion of the polymer and solvent coexist in homogeneous mixtures with a hydrogen-bonded polar solvent and a polymer.

PVP is soluble not only in hydrogen-bonding liquids such as alcohols and water but also in chloroform, a weaker polar solvent. The static dielectric constant of chloroform is 4.72, and chloroform has a dielectric relaxation process, whose relaxation time and strength are 5.9 ps and 2.6 at 25 °C.[22] The relaxation strength of chloroform is much weaker than those of alcohols and water, and its relaxation time is close to that of water; thus, we can clearly observe the relaxation process of the segmental motion of PVP. Although the relaxation process of the segmental motion of PVP has been observed in alcohol and water mixtures, the large contributions of dc conductivity and the relaxation process of the alcohol and water to dielectric spectra make it difficult to discuss the PVP relaxation process in detail. Therefore, chloroform is useful for investigating the chain dynamics of PVP. Understanding of the dynamics of water-soluble polymers with stronger polar groups is expected to bring about considerable progress for the knowledge of not only various water-soluble polymers but also biomacromolecules, for example, the relationship between the conformational fluctuation of proteins and their functions. In addition, it is worth comparing the dynamics of PVP with those of polymers in nonpolar organic solvents, which have been investigated extensively in polymer physics.

## EXPERIMENTAL SECTION

PVP with average molecular weights $M_w/(\mathrm{g\ mol^{-1}})$ of approximately $1 \times 10^4$, $4 \times 10^4$, and $3.6 \times 10^5$ and chloroform were purchased from Sigma. Mixtures of PVP ($M_w = 4 \times 10^4$) in chloroform were prepared without further purification with various PVP concentrations from 5 to 35 wt % with an accuracy better than 0.05 wt %. PVP−chloroform mixtures of 5 wt % PVP with approximately $M_w = 1 \times 10^4$ and $3.6 \times 10^5$ were prepared to study the PVP molecular weight dependence of the relaxation of PVP. Prior to mixing, PVP was kept in a dry atmosphere in a desiccator with $P_2O_5$.

Dielectric measurements were performed in a frequency range from 20 mHz to 1.8 G Hz and at temperatures between 123.2 and 298.2 K using an alpha dielectric analyzer (Novocontrol, 20 mHz−3 MHz), a precision impedance analyzer (Agilent Technologies 4294A, 40 Hz−110 MHz), and an impedance/material analyzer (Hewlett-Packard 4291A, 1 MHz−1.8 GHz). The viscous polymer solution and silica spacers with a diameter of 50 $\mu$m were sandwiched between brass plate electrodes for the dielectric measurement using the alpha dielectric analyzer. A coaxial cylindrical sample cell with a geometrical capacitance of 0.20 pF was connected to the DUT port (APC 7 coaxial connector) of the test head through a semirigid coaxial line with 25 cm length. This arrangement was used for the measurements using the precision impedance analyzer and impedance/material analyzer.

Chloroform has a melting temperature, $T_m$, of 210 K; thus, all mixtures except for the 35 wt % PVP−chloroform mixture were crystallized below $T_m$. For the 35 wt % PVP−chloroform mixture, the large amount of polymer in the mixture prevents the crystallization of chloroform. In this paper, we focus on the dynamics of polymer solution in which the chloroform did not crystallize; thus, we only present results above $T_m$.

## RESULTS

We performed dielectric measurements on 5 wt % PVP−chloroform mixtures with PVP molecular weights of approximately $1 \times 10^4$, $4 \times 10^4$, and $3.6 \times 10^5$ at 298.2 K. The frequency, $f$, dependences of the real ($\varepsilon'$) and imaginary ($\varepsilon''$) parts of the dielectric functions of the 5 wt % PVP−chloroform mixtures are shown in Figure 2. The relaxation process of PVP can be observed, its loss peak frequency shows no PVP molecular weight dependence, and only the contributions of dc conductivity at lower frequencies varied. Combined with the characteristic properties of the relaxation process of PVP observed in alcohol and water mixtures,[5] this relaxation process can be considered to originate from the segmental motion of PVP. We call this relaxation process "the PVP process".

Figure 3 shows the frequency dependences of the real and imaginary parts of the dielectric functions for a 30 wt % PVP−chloroform mixture with PVP of approximately $M_w = 4 \times 10^4$ at various temperatures. The PVP process can be clearly seen in both the real and imaginary parts at all temperatures. The low-frequency tail of the relaxation process of chloroform is observed at frequencies above 100 MHz in the imaginary part of the dielectric function (Figure 3b,c), but its loss peak cannot be observed in the frequency range measured. The relaxation of chloroform has relatively low strength. The high-frequency portion of electrode polarization is observed below 100 Hz at 293.2 K and below 1 Hz at 223.2 K in the real parts (Figure 3a), and the contribution of dc conductivity is observed on the low-frequency side of the loss peak of the PVP process (Figure 3b).

To characterize the relaxation processes, curve fitting was carried out. The dielectric constants and losses for the PVP−chloroform mixtures with various concentrations and at various

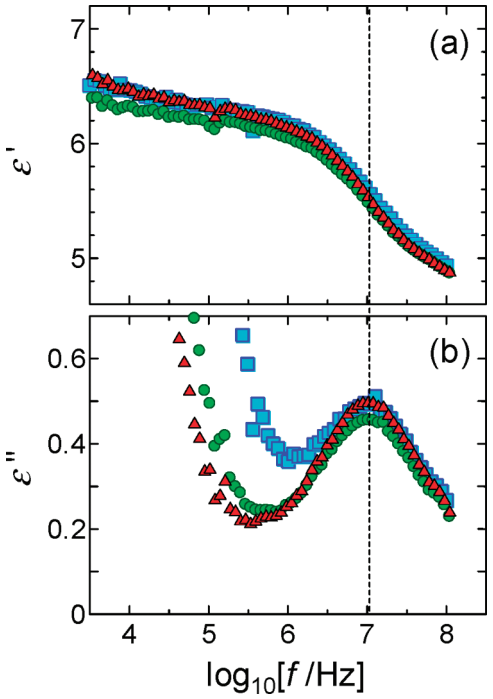


**Figure 2.** Real (a) and imaginary (b) parts of dielectric functions of 5 wt % PVP−chloroform mixtures with various molecular weights of PVP at 298.2 K. Blue squares, green circles, and red triangles indicate PVP molecular weights of approximately $1 \times 10^4$, $4 \times 10^4$, and $3.6 \times 10^5$, respectively. The dashed vertical line indicates the loss peak frequency.

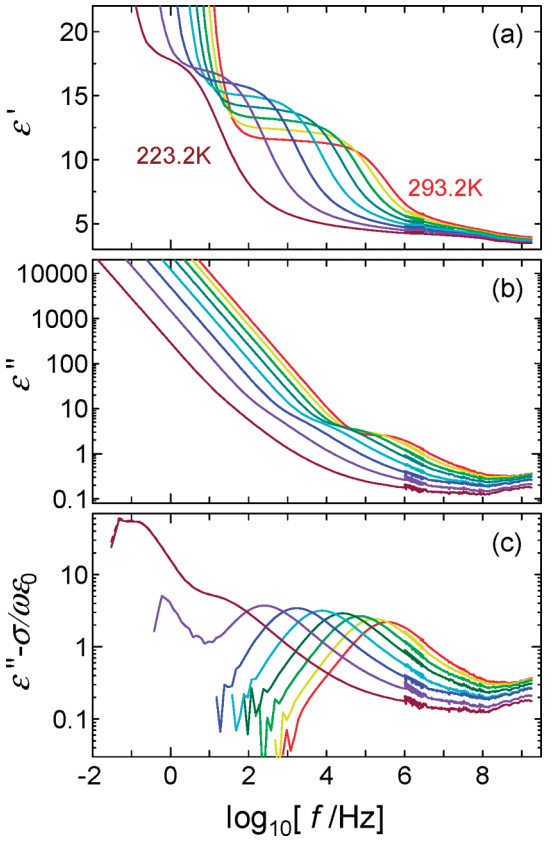


**Figure 3.** Real (a) and imaginary (b) parts of dielectric functions of 30 wt % PVP−chloroform mixture (PVP with approximately $M_w = 4 \times 10^4$) at various temperatures from 223.2 to 293.2 K in steps of 10 K. (c) Imaginary parts of dielectric functions from which the contributions of dc conductivity have been subtracted. The dc conductivity of each dielectric loss was estimated at frequencies between 2 and 3 orders of magnitude lower than the loss peak frequency.

temperatures can be described as a simple sum of four relaxation processes and a contribution of dc conductivity. The PVP process can be described by the asymmetric Havriliak−Negami (HN) equation.[23] The relaxation process of chloroform on the higher-frequency side and the high-frequency portion of electrode polarization on the lower-frequency side of our frequency window were fitted by the symmetric Cole−Cole equation.[24] The dielectric functions are described as

$$\varepsilon^*(\omega) = \varepsilon_\infty + \frac{\Delta\varepsilon_{Chl}}{1+(j\omega\tau_{Chl})^{\beta_{Chl}}} + \frac{\Delta\varepsilon_S}{1+(j\omega\tau_S)^{\beta_S}} + \frac{\Delta\varepsilon_{PVP}}{\{1+(j\omega\tau_{HN})^{\beta_{PVP}}\}^{\alpha_{PVP}}} + \frac{\Delta\varepsilon_{EP}}{1+(j\omega\tau_{EP})^{\beta_{EP}}} - j\frac{\sigma}{\varepsilon_0\omega} \quad (1)$$

where $\omega$ is the angular frequency, $j$ is the imaginary unit given by $j^2 = -1$, $\varepsilon_0$ is the dielectric constant in vacuum, $\varepsilon_\infty$ is the limiting high-frequency dielectric constant, $\Delta\varepsilon$ is the relaxation strength, $\tau$ is the relaxation time, $\tau_{HN}$ is the relaxation time given by the HN equation, $\alpha$ and $\beta$ are the asymmetric and symmetric broadening parameters ($0 < \alpha, \beta \leq 1$), respectively, and $\sigma$ is the dc conductivity. The subscripts Chl, PVP, and EP denote the relaxations of chloroform, PVP, and electrode polarization, respectively. The subscript S denotes the small relaxation between the PVP and chloroform processes. The contribution of dc conductivity is given by the sixth term on the right-hand side of eq 1. The relaxation times of the PVP process were determined directly from the loss peak frequencies, $f_p$, by the relation $\tau = 1/(2\pi f_p)$. $\tau$ in the Cole−Cole equation agrees with the relaxation time obtained from the loss peak frequency. On the other hand, $\tau_{HN}$ obtained by eq 1 differs from $\tau = 1/(2\pi f_p)$;[25] thus, $\tau_{HN}$ was not used in the discussion. The relaxation time obtained from the loss peak frequency is independent of the model used and the most probable relaxation time. The loss peaks of the electrode polarization and the relaxation of chloroform were outside the low- and high-frequency limits of our measurements; thus, the relaxation parameters of these processes are inaccurate. We cannot assert that there is no other relaxation process in the frequency range between the PVP and chloroform processes, since the curve given by eq 1 without the S process could not reproduce the frequency range shown by the gray dashed curve in Figure 4. The origin of the S process is expected to be the secondary relaxation of PVP or the relaxation process of the small amount of residual water in dry PVP. However, its strength is very low, and the relaxations of PVP and chloroform prevent the detailed characterization of the small S process. Therefore, only the relaxation parameters of the PVP process are reliable and we will discuss the PVP process only in this paper.

The loss peak of the PVP process is covered by the contribution of dc conductivity at lower temperatures. To characterize the shape of the loss peak of the PVP process, the contribution of dc conductivity was subtracted from the loss spectra. $\sigma$ for each dielectric loss spectrum was estimated in four frequency ranges of 1.5−2.5, 2−3, 2.5−3.5, and 3−4 orders of magnitude lower than the loss peak frequency. The contribution of dc conductivity determined from the four values of $\sigma$ were subtracted from the loss spectra. Figure 4 shows examples of the loss spectra, from


dx.doi.org/10.1021/ma102394s |*Macromolecules* 2011, 44, 2140–2148

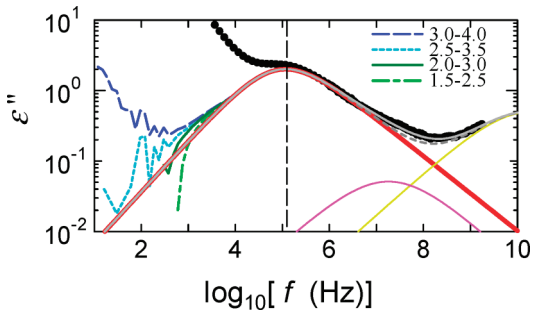


**Figure 4.** Dielectric loss spectra of 20 wt % PVP−chloroform mixture (PVP with approximately $M_w = 4 \times 10^4$) at 253.2 K (black circles) were each from which the contributions of dc conductivity determined by four values of $\sigma$ subtracted. $\sigma$ was estimated at frequency ranges of 1.5−2.5 (light green dot-dash line), 2−3 (green solid line), 2.5−3.5 (cyan dashes line), and 3−4 (blue dashes line) orders of magnitude lower than the loss peak frequency (vertical dashed line) to be 1.643, 1.638, 1.636, and 1.634 $\mu$S/m, respectively. Red and yellow solid curves are the relaxation processes of PVP and chloroform, respectively. The magenta solid line is the S process. The summation of the PVP and chloroform processes without the S process is given by the gray dashed curve. The sum of the PVP, chloroform, and S processes is given by the gray solid curve.

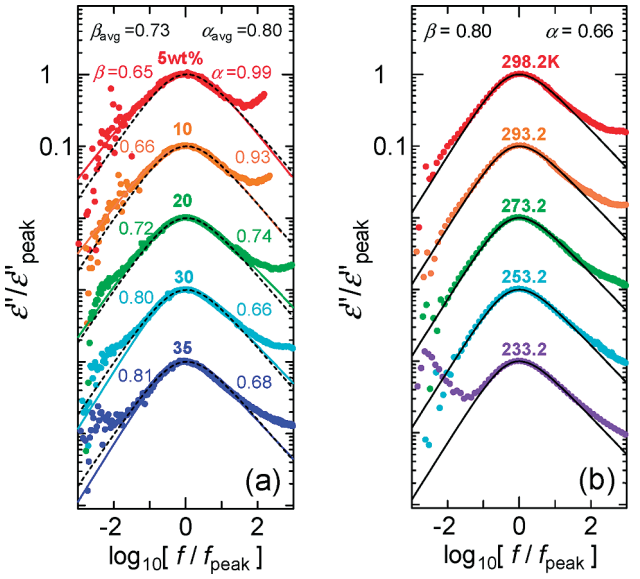


**Figure 5.** Normalized loss peak of the PVP process from which the contributions of dc conductivity were subtracted for the PVP−chloroform mixtures (PVP with approximately $M_w = 4 \times 10^4$). The plots are experimental results, and the concentrations and temperatures are presented above the loss peak. The values on the vertical axis of the plots obtained for different concentrations and temperatures have been shifted by orders of magnitude for clarity. (a) PVP−chloroform solutions with various concentrations at 298.2 K. The values of $\alpha_{avg}$ and $\beta_{avg}$ at the top of the figure are the averages obtained from the loss peaks of all concentrations and temperatures. The dashed curves were obtained from the H−N equation with $\alpha_{avg} = 0.80$ and $\beta_{avg} = 0.73$. The values of $\alpha$ and $\beta$ respectively presented to the right and left of each concentration are average values obtained for all the temperatures, and the curves drawn using these values are shown as solid lines. (b) 30 wt % PVP−chloroform solution at various temperatures. The solid lines were obtained from the H−N equation with values of $\alpha = 0.66$ and $\beta = 0.80$, which are the averages obtained from the loss peak of all temperatures for the 30 wt % PVP solution.

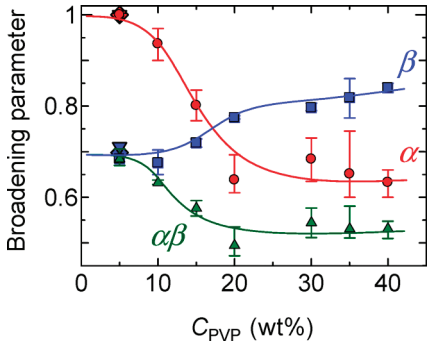


**Figure 6.** Plots of the broadening parameters, the asymmetric parameter $\alpha$ (red circles), the symmetric parameter $\beta$ (blue squares), and $\alpha\beta$ (green triangles), against concentration of PVP $C_{PVP}$ (wt %) for PVP−chloroform mixtures of PVP with approximately $M_w = 4 \times 10^4$ at 298.2 K. Diamonds and invert triangles are the plots obtained for the 5 wt % PVP−chloroform mixtures of PVP with approximately $M_w = 1 \times 10^4$ and $3.6 \times 10^5$, respectively.

which contributions of dc conductivity obtained from the four values of $\sigma$ were each subtracted. For the loss spectra in the frequency range down to 1.5 orders of magnitude lower than that of the loss peak of the PVP process, the four loss spectra are in agreement with each other. Therefore, we use loss spectra in this frequency range to discuss the shape of the PVP process. The loss spectra of 30 wt % PVP−chloroform mixtures at various temperatures, from which the contributions of dc conductivity estimated in the frequency range of 2−3 orders of magnitude lower than the loss peak frequency of the PVP process were subtracted, are shown in Figure 3c. At 293.2 K, we can estimate the shape of the lower frequency side of the loss peak down to frequencies 2 orders of magnitude lower than that of the loss peak. However, for example, at 233.2 K, we can observe the tail of the loss peak down to frequencies 1 order of magnitude lower than that of the loss peak.

Figure 5a shows the loss peak of the PVP process normalized by the loss peak height and frequency in PVP−chloroform mixtures with various concentrations at 298.2 K. Figure 5b shows the normalized loss spectra of the 30 wt % PVP−chloroform mixture at various temperatures. All the loss peaks at various temperatures almost lie on a single trace as shown in Figure 5b. The asymmetry of the loss peaks increases with increasing PVP concentration as shown in Figure 5a. It can be concluded that the shape of the loss peak of the PVP process depends on the polymer concentration, but it is independent of temperature. Therefore, the estimated PVP concentration dependence of the shape parameters at 298.2 K is expected to be the same for all the temperature measured. Figure 6 shows plots of the broadening parameters $\alpha$, $\beta$, and $\alpha\beta$ against PVP concentration at 298.2 K. $\alpha$ decreases and $\beta$ increases with increasing PVP concentration. In the mixtures with lower PVP concentrations, the shape is symmetrically broadened and almost Cole−Cole type. On the other hand, in the mixtures with higher PVP concentration, the shape is asymmetrically broadened.

Figure 7 shows plots of relaxation strength against reciprocal temperature. The relaxation strength increases linearly with decreasing temperature, and the temperature dependences are stronger than those expected by the proportionality in $1/T$ for all the mixtures. There are a lot of literatures on the theory and practice of the dependence of $\Delta\varepsilon$ on magnitude and density of

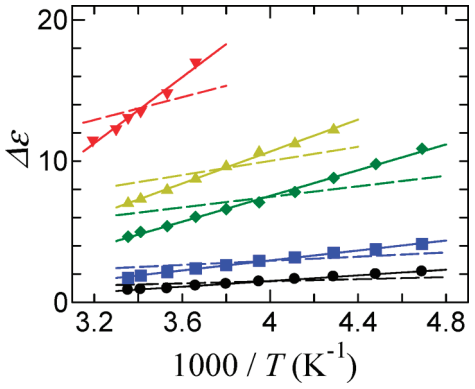


**Figure 7.** Temperature dependences of relaxation strength, $\Delta\varepsilon$, of the PVP process at various concentrations for PVP−chloroform mixtures of PVP with approximately $M_w = 4 \times 10^4$. The black circles, blue squares, green diamonds, yellow triangles, and red inverted triangles indicate 5, 10, 20, 30, and 35 wt % PVP, respectively. The solid and dashed lines were obtained by least-squares fitting assuming a linear dependence of $1/T$. When plotting the dashed lines, it was assumed that $\Delta\varepsilon = 0$ at $1/T = 0$.

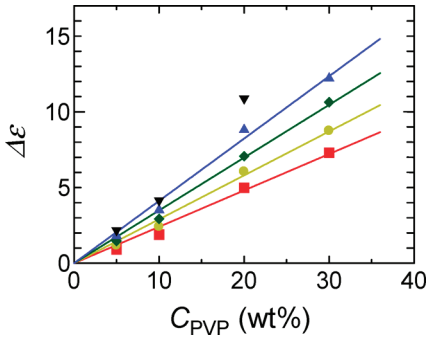


**Figure 8.** PVP concentration, $C_{PVP}$, dependence of relaxation strength, $\Delta\varepsilon$, at various temperatures for PVP−chloroform mixtures of PVP with approximately $M_w = 4 \times 10^4$. The black inverted triangles, blue triangles, green diamonds, yellow circles, and red squares indicate 213.2, 233.2, 253.2, 273.2, and 293.2 K, respectively. The lines were drawn by least-squares fitting by assuming linear concentration dependences of $\Delta\varepsilon$.

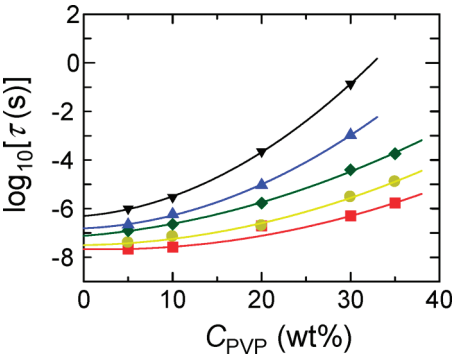


**Figure 9.** PVP concentration, $C_{PVP}$ (wt %), dependence of relaxation time, $\tau$, of PVP process at various temperatures for PVP−chloroform mixtures of PVP with approximately $M_w = 4 \times 10^4$. The black inverted triangles, blue triangles, green diamonds, yellow circles, and red squares indicate 213.2, 233.2, 253.2, 273.2, and 293.2 K, respectively. The lines were drawn by least-squares fitting by assuming linear dependences of $\log[\tau\ (s)]$ on the square of the concentration of PVP (wt %).

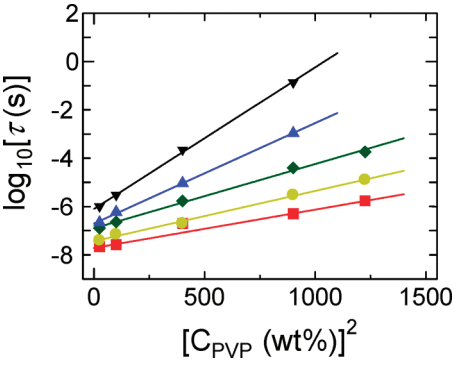


**Figure 10.** Plots of logarithm of relaxation time, $\tau$, of the PVP process against square of PVP concentration, $[C_{PVP}\ (\text{wt}\,\%)]^2$, at temperatures of 213.2, 233.2, 253.2, 273.2, and 293.2 K, shown by black inverted triangles, blue triangles, green diamonds, yellow circles, and red squares, respectively, for PVP−chloroform mixtures of PVP with approximately $M_w = 4 \times 10^4$. The lines were drawn by assuming linear dependences of $\log[\tau\ (s)]$ on $[C_{PVP}\ (\text{wt}\,\%)]^2$.

dipole moment, the Kirkwood $g$-factor, internal electric field, and temperature for various systems including polymers.[25−31] The strong temperature dependence of $\Delta\varepsilon$ is expected to be due to the change of the Kirkwood $g$-factor originated in the increase of interchain interactions that increase the magnitude of the effective dipole moment with decreasing temperature. The change of the permittivity of chloroform with temperature is also expected the cause of the strong temperature dependence. Figure 8 shows plots of relaxation strength against concentration of PVP, $C_{PVP}$, at several temperatures. The strength is almost proportional to the PVP concentration at all the temperatures measured. In this concentration range, the strength of the PVP process is determined simply by the density of the dipole moment on the PVP chain in the mixtures at constant temperature.

Figure 9 shows the PVP concentration dependence of relaxation time at several temperatures. The concentration dependence is stronger at lower temperatures. Figure 10 shows plots of relaxation time against the square of PVP concentration. The relaxation time depends linearly on the square of PVP concentration. In dilute solutions of a polymer, the relaxation time is determined by the solvent viscosity,[3,5,32−34] which is discussed below. On the other hand, the linear dependence of the relaxation time on the square of PVP concentration could be expected that the relaxation time is a function of the second virial coefficient. Then, the excluded volume effect between polymer chains, i.e., the interchain interaction of the polymer, generates the main friction causing the increase in relaxation time with PVP concentration.

Figure 11 shows plots of relaxation time against reciprocal temperature for mixtures with various concentrations. The temperature dependences of relaxation time for the mixtures with 20, 30, and 35 wt % PVP are well described by the Vogel−Fulcher−Tammann−Hesse (VFTH) equation, given by[35,36]

$$\log \tau = \log \tau_\infty + \frac{B}{T - T_0} \qquad (2)$$

where $\tau_\infty$ (the relaxation time at an infinite temperature), $B$, and $T_0$ are the VFTH parameters. The ranges of temperature and relaxation time are not sufficiently wide to obtain the VFTH

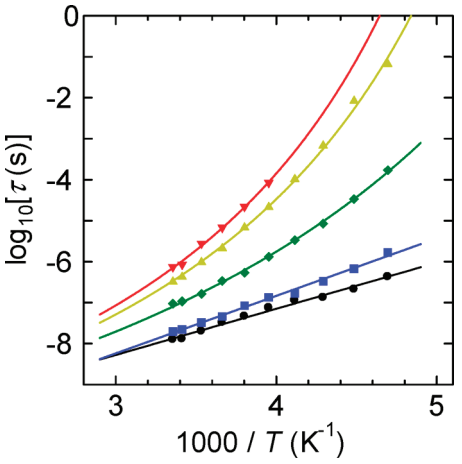


**Figure 11.** Temperature dependences of logarithm of relaxation time, $\tau$, of the PVP process observed for PVP−chloroform mixtures (PVP with approximately $M_w = 4 \times 10^4$) with PVP concentrations of 5, 10, 20, 30, and 35 wt % represented by black circles, blue squares, green diamonds, yellow triangles, and red inverted triangles, respectively. Curves for the plots of 20, 30, and 35 wt % PVP−chloroform mixtures were obtained by least-squares fitting using the VFTH equation given by eq 2, and the straight lines for the plots of 5 and 10 wt % PVP−chloroform mixtures were obtained by least-squares fitting.

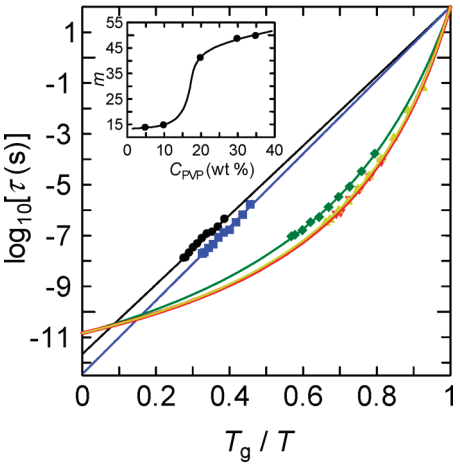


**Figure 12.** Plots of $\log[\tau\ (s)]$ of the PVP process against reciprocal temperature normalized by $1/T_g$ for PVP−chloroform mixtures of PVP with approximately $M_w = 4 \times 10^4$. $T_g$ is the temperature at which the relaxation time of the PVP process is 100 s. The black circles, blue squares, green diamonds, yellow triangles, and red inverted triangles represent PVP concentrations of 5, 10, 20, 30, and 35 wt %, respectively. Curves for the plots of 20, 30, and 35 wt % PVP−chloroform mixtures were obtained by least-squares fitting using the VFTH equation given by eq 2, and the straight lines for the plots of 5 and 10 wt % PVP−chloroform mixtures were obtained by least-squares fitting. The inset is plots of fragility, $m$, against PVP concentration, $C_{PVP}$ (wt %).

**Table 1. VFTH Parameters, Glass Transition Temperature, and the Fragility of the PVP Process in PVP−Chloroform Mixtures**[a]

| PVP concn (wt %) | $T_0$ (K) | $B$ (K) | $T_g$ (K) | $m$ |
|---|---|---|---|---|
| 20 | 116 | $6.8 \times 10^2$ | 169 | 41 |
| 30 | 145 | $6.7 \times 10^2$ | 197 | 49 |
| 35 | 152 | $6.8 \times 10^2$ | 206 | 50 |

[a] $\log[\tau_\infty] = -10.84$ was used for all concentrations.

parameters for 5 and 10 wt % PVP−chloroform mixtures, since the crystallization of chloroform at 210 K interferes with the observation of the PVP process near its $T_g$ at lower temperatures. In this temperature range, the temperature dependences of the relaxation time for the mixtures with 5 and 10 wt % of PVP are the Arrhenius type. The value of $\log \tau_\infty = -10.84$ was obtained by averaging $\log \tau_\infty$ for 10, 20, and 30 wt % PVP−chloroform mixtures, whose relaxation times could be determined over rather wide frequency and temperature ranges. We fixed $\log \tau_\infty = -10.84$ for 20, 30, and 35 wt % PVP−chloroform mixtures. This concentration-independent $\log \tau_\infty$ is based on the trend of local chain motion of polymers in a nonpolar solvent.[28,29,37] The VFTH parameters are consistent with those obtained in polymer solutions of a nonpolar solvent. The glass transition temperatures obtained from eq 2 with a relaxation time of the PVP process of 100 s are listed in Table 1. Even though the solutions crystallize below 210 K and the solutions never reach their $T_g$ in reality, we introduced the VFTH parameters and $T_g$ for the characterization of the temperature dependence of the relaxation time.

Fragility, which measures the extent of the deviation from the Arrhenius temperature dependence, has been used to classify the temperature dependence of relaxation time and viscosity in relation to the α process in various glass formers.[38] Figure 12 shows plots of relaxation time against reciprocal temperature normalized by $1/T_g$. The curvature of the plots is greater, i.e., more fragile, for higher PVP concentrations. The fragility index, $m$, is the value of the slope in Figure 12 at $T_g/T = 1$, where

$$m = \frac{\mathrm{d}[\log \tau]}{\mathrm{d}(T_g/T)_{T=T_g}} \tag{3}$$

From the VFTH equation and eq 3, the value of $m$ is obtained from $B$, $T_0$, and $T_g$ as

$$m = \frac{B}{T_g\left(1 - \left(\frac{T_0}{T_g}\right)\right)^2} \tag{4}$$

The values of $m$ obtained this way are listed in Table 1 and plotted on the inset in Figure 12. $m$ smaller than ∼15 is the Arrhenius temperature dependence of relaxation time. The values of $m$ are larger in higher PVP concentration. The composition dependence of fragility in two-component systems of miscible polymer blends and polymer/small-molecule solutions has been reported.[39] For PVP−chloroform mixtures, two relaxations due to the molecular motion of chloroform and the segmental relaxation of PVP occur separately. This implies that the degree of coupling of the mobility between PVP segments and chloroform molecules appears to be weak. In this case, the increase in fragility with PVP concentration reflects the increase in friction due to the interchain interaction of PVP.

## DISCUSSION

**Chain Motion of PVP with Respect to Solvent Viscosity.** The PVP process has previously been observed in PVP−water and PVP−normal alcohol mixtures[5] as well as in PVP−EGO mixtures.[3] The relaxation time of the PVP process at zero

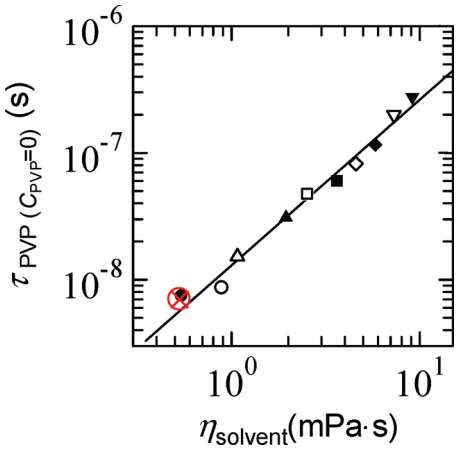


**Figure 13.** Plots of relaxation time of the PVP process at $C_{PVP}$ = 0 wt % in PVP solutions (PVP with approximately $M_w = 4 \times 10^4$) with various solvents at 298.2 K. The red circle with a cross, solid circle, open circle, open triangle, solid triangle, open square, solid square, open diamond, solid diamond, open inverted triangle, and solid inverted triangle represent mixtures of PVP and chloroform, water, methanol, ethanol, 1-propanol, 1-butanol, 1-pentanol, 1-hexanol, 1-heptanol, 1-octanol, 1-nonanol, and 1-decanol, respectively. The solid line was obtained by least-squares fitting.

polymer concentration, $\tau_{PVP(C=0)}$, was obtained from plots of the relaxation time of PVP, $\tau_{PVP}$, against PVP concentration, $C_{PVP}$, by extrapolation from those observed in PVP solutions to the value for pure solvent, $C_{PVP}$ = 0. The extrapolation was carried out using eq 2 in ref 5. $\tau_{PVP(C=0)}$ implies the relaxation time of an isolated PVP molecule in an infinitely dilute solution of PVP. Plots of $\tau_{PVP(C=0)}$ against solvent viscosity, $\eta_S$, of pure solvents of PVP−alcohol mixtures at 25 °C are from ref 5. The line obtained by least-squares fitting indicated the relationship $\tau_{m0} \propto \eta_S^{1.3}$ for PVP−alcohol and PVP−water mixtures.[5] On the basis of the Debye−Stokes equation,[40] the relationship between the relaxation time of the local chain motion of an isolated polymer and the viscosity of solvent, $\eta_S$, has been discussed.[27] According to the Debye−Stokes equation,[40] this relationship is given by

$$\tau_{polymer} = \frac{V\eta_S}{k_B T} \quad (5)$$

where $k_B$ is the Boltzmann constant, $V$ is the effective volume of a moving unit, and $T$ is absolute temperature. The relationship between $\tau_{polymer}$ and $\eta_S$ has been studied experimentally and is given by $\tau_{polymer} \propto \eta_S^n$, and values of $n$ have been obtained in the range of 0.74−1.3.[3,5,32−34] The local chain motion of PVP in alcohol and water solutions can be regarded as motion in homogeneous viscous media, similarly to the local chain motion of a polymer in a nonpolar solvent, in spite of the existence of hydrogen bonds between PVP and alcohol or water molecules. The plot of $\tau_{PVP}$ vs $\eta_S$ for PVP−chloroform mixture at 298.2 K is added to Figure 13. Note that regardless of the polarity and hydrogen-bonding ability of the solvent, the plot of $\tau_{PVP}$ vs $\eta_S$ for PVP−chloroform mixture is almost on the line obtained from the PVP−alcohol and PVP−water mixtures. We thus confirmed that the PVP process observed in PVP−chloroform mixtures involves the segmental motion of PVP with the same origin as those observed in PVP−water, PVP−alcohol, and PVP−EGO mixtures.[3,5]

**Concentration and Temperature Dependences of Relaxation Time of the PVP Process.** The VFTH parameters listed in Table 1 are in the ranges of values previously obtained for the segmental motion of a polymer in nonpolar solvents. We assumed a constant value of $\log[\tau_\infty]$ since the value of $\log[\tau_\infty]$ obtained for the relaxation process of the local chain motion of a polymer in various polymer−nonpolar solvent solutions is independent of polymer concentration.[28,29,37] The value of $B$ in eq 2 for the relaxation of the local chain motion of a polymer in a nonpolar solvent is also independent of polymer concentration.[28,29,37] For the PVP process in PVP−chloroform mixtures, the values of $B$ are in the range of 6.7−6.8 × $10^2$ K. This variation is within the range of experimental error since the relaxation times were obtained in rather narrow temperature and frequency ranges. Therefore, we conclude that the values of $B$ are almost constant.

The fragility increases with increasing polymer concentration. This is also true for the relaxation of the segmental motion of a polymer in a nonpolar solvent estimated by dielectric measurements over wide temperature and frequency ranges.[28,29,37,39,41] The relaxation time increases with increasing polymer concentration, and $\log[\tau]$ exhibits a roughly linear dependence on the square of polymer concentration as shown in Figure 10. This can be interpreted to mean that the interchain interaction of polymer chains in the mixture determines the shift factor from $\tau_{PVP(C=0)}$ to $\tau_{PVP}$. In a dilute solution, the interchain interaction of polymer chains is low. In this case, the relaxation time obeys the Arrhenius temperature dependence, since the large amount of chloroform solvent reduces the interchain cooperativity of the segmental motion, mainly due to the exclusive volume effect among PVP chains, even at lower temperatures. On the other hand, in mixtures with higher polymer concentrations, the larger polymer density results in larger interchain interactions of the polymer. In this case, the cooperativity of the polymer chain increases with decreasing temperature, which results in an increase in the apparent activation energy. This is why the fragility is larger at higher polymer concentrations in all the polymer solutions measured.

**Shape of the Dielectric Loss of the PVP Process.** The shape of the dielectric loss of the segmental relaxation of polymers in solutions has been discussed so far for polymer mixtures with nonpolar and weak polar solvents. The dependences on temperature and composition are affected by the interactions of polymer and solvent molecules in the mixtures. For concentrated solutions of poly(vinyl acetate) (PVAc) in 1-methylnaphthalene (MN) and poly(vinyl octanoate) (PVOc) in toluene (Tol), the relaxation spectra of the segmental motion of the polymer are much broader than those in neat and dilute PVAc.[28] The relaxation spectra observed in neat and dilute PVAc are independent of temperature, and the symmetric and asymmetric H−N broadening parameters are 0.882 and 0.526. On the other hand, the relaxation spectra of concentrated solutions broaden with decreasing temperature near the glass transition temperature. The breadth of the relaxation spectra decreases in the order PVAc/Tol, PVAc/MN, PVOc/Tol at the same $T/T_g$. The broadening behavior is also explained by assuming that the breadth is proportional to the amplitude of the local concentration fluctuation.[28] The dielectric relaxation of concentrated solutions of polystyrene (PS) in toluene (30−70 wt % PS), ethylbenzene (EtBz), *n*-propylbenzene (PrBz), and *n*-butylbenzene (BuBz) (30−40 wt % PS with EtBz, PrBz, BuBz) were previously studied.[37] The half-width of the dielectric loss curve, $\Lambda_\alpha$, for the α relaxation for solutions in EyBz, PrBz, and BuBz

increases with decreasing temperature (similarly to in PVAc−Tol solution). In contrast, the value of $\Lambda_\alpha$, i.e., the shape of the dielectric loss spectra of PS in toluene solutions, is independent of composition and temperature at 30−70 wt % PS. Depolarized Rayleigh scattering and dielectric spectroscopy were employed to study the solvent and polymer dynamics in PS/Tol systems 0−0.6 g/mL PS.[41] The shape parameters of the Kohlrausch function are $\beta_{KWW,slow} = 0.41$ and $\beta_{KWW,fast} = 0.2$ for the slow (segmental motion of PS) and fast processes (relaxation of toluene) in a PS/Tol system, respectively. The shape parameters are $\beta_{KWW,PS} = 0.4$ in neat PS and $\beta_{KWW,tol} = 0.5$ in neat toluene at $T_g$. The shape of the segmental relaxation spectra of PS in the solution is the same as that of the spectra for neat PS, but the shape of the relaxation spectra of toluene in a polymer solution is much broader than that of neat toluene. PS in toluene is special among the systems examined so far in the sense that toluene is almost a perfect good solvent for PS.[42] The dielectric relaxation process of mixtures of 2,6-dihydroxynaphthalene/poly(vinyl ethyl ether) (DHN/PVEE) containing 1−20 wt % DHN was previously investigated.[39] A single cooperative segmental relaxation was observed for all mixtures. The breadth of the α relaxation was found to be independent of temperature and composition. However, the range of concentration was narrow, making it difficult to determine the concentration dependence of the breadth. A single cooperative segmental relaxation has also been observed in globally miscible poly(4-vinylphenol) [PVPh]−PVEE blends containing 30−50 wt % PVPh, whereas blends with less than 30% PVPh exhibit two segmental processes.[43] These PVPh/PVEE blends with high PVPh content exhibit thermorheological simplicity with a relaxation breadth that changes with composition but not with temperature.

The shape of the relaxation spectra for the PVP process in chloroform mixtures with 20 wt % PVP and higher concentrations is independent of temperature as shown in Figure 5b. The dielectric relaxation strength of the PVP process is the largest in those of the segmental motion of random coiled polymers in solutions. This means that the magnitude of the dipole moment of a repeat unit of PVP is the largest in the polymers mentioned above, and the electrostatic interaction between PVP and chloroform is the strongest. In this case, PVP molecules are extended by their mutually repulsive force in the good solvent of chloroform. The extended PVP molecules form a homogeneous mixture. The temperature-independent shape of the loss peak, namely, the time−temperature superposition (TTS), is satisfied. Generally, the TTS is satisfied for neat materials. On the other hand, in various mixtures and polymer blends, the TTS is not satisfied owing to concentration fluctuation. In the polar PVP−chloroform mixtures, the strong electrostatic repulsive force among the PVP chain prevents the concentration from fluctuating, and the mixture is expected to be spatially homogeneous.

$\beta$ is smaller, i.e., the symmetric broadening is larger, in the mixtures with lower PVP concentrations. The origin of the symmetric broadening is expected to be different from that of asymmetric broadening. Symmetric broadening is observed for the local secondary relaxation, the relaxation of the solvent in polymer solutions, and also the relaxation in polymer blends. The variation of local conditions can cause the symmetric broadening of the loss peak of dielectric relaxation. As mentioned in ref 28, the broadening of the loss peak with decreasing temperature can be explained by assuming that the distribution of relaxation time is proportional to the magnitude of the heterogeneity due to concentration fluctuation. According to Figure 11 in ref 28, the concentration dependence of relaxation time increases with decreasing temperature. This trend also appears in the plots shown in Figure 9. This is why the concentration variation in the mixture induces the broadening of relaxation time at lower temperatures. Note that the broadening was large on the low-frequency side of the loss peak, as shown in Figure 7 of ref 28. For 5 and 10 wt % PVP−chloroform mixtures, the low-frequency side of the loss peak of the PVP process is broader than those observed for the mixtures with 20 wt % and higher PVP concentrations, as shown in Figure 5a. It is expected that the broadening of the low-frequency side of the PVP process is caused by the concentration fluctuation, as mentioned above, and that the breadth of the PVP process increases with decreasing temperature. However, we could not confirm this point for the mixtures with 5 and 10 wt % PVP since the temperature and frequency ranges in which the PVP process could be observed were narrow. For the mixtures of such lower PVP concentrations, the local composition is expected to be heterogeneous, since the chain connectivity in PVP molecules results in a PVP-rich region around PVP molecules. The PVP molecules cannot fill the spaces in the solution; thus, there are chloroform-rich regions. On the other hand, the symmetric broadening is smaller in the mixtures with higher PVP concentrations.

It had been reported that the fragility is related to the shape of the loss peak of the α process in neat glass formers. The coupling model predicted that their relationship depends on the strength of the cooperativity of moving units.[44] The stronger coupling of molecular motion bring results in larger values of $m$ and the coupling constant $n$, where $n$ is related to the stretched exponent of the time-dependent Kohlrausch relaxation function as $n - 1 = \beta_{KWW}$. The fragility increases with increasing PVP concentration, and the asymmetry, which is represented by the deviation of the asymmetric HN shape parameter α from unity, increases with PVP concentration. These two behaviors are consistent with the increase in the cooperativity of the segmental motion of PVP with increasing PVP concentration.

For various polymer solutions, both the concentration fluctuation and the cooperativity of molecular motion contribute to the broadening of the loss spectra of the segmental relaxation of the polymer chain. In such cases, no clear relationship has been observed between the broadening and the fragility of the relaxation due to the segmental motion of the polymer. For the homogeneous polymer solution of PVP−chloroform, the asymmetric broadening of the loss peak and the fragility are related, since both of them originate from the cooperativity of the segmental motion of the polymer chain. In the case of a polymer in water, the polarities of the water and polymer are strong compared with those of nonpolar solvent polymer solutions. Therefore, it is expected to be universally true that polymer−water mixtures are rather homogeneous if water is a good solvent of the polymer.

## ■ CONCLUSION

Broadband dielectric measurements of PVP−chloroform mixtures with PVP concentrations from 5 to 35 wt % at temperatures between 298 and 210 K were performed in the frequency range of 20 mHz−1.8 GHz. The dielectric relaxation process due to the segmental motion of PVP is characterized to be that of hydrophilic polymers. We obtained the following results. (i) The temperature and concentration dependences of the mean relaxation time of the PVP process are comparable to

those observed in nonpolar and weakly polar polymer solutions. (ii) The loss spectrum of the PVP process is broadened asymmetrically, and the relaxation time obeys VFTH temperature dependence for the mixtures with 20 wt % PVP and higher. On the other hand, the loss spectrum of the PVP process is symmetrical in shape, and its relaxation time obeys the Arrhenius type for the mixtures with 10 wt % PVP and lower. (iii) The shape of the loss spectrum changes with PVP concentration owing to the increase of cooperativity of the segmental motion of PVP with PVP concentration. On the other hand, the TTS is satisfied, namely, the asymmetric shape of the loss spectrum does not change with temperature for the mixtures with 20 wt % PVP and higher. This is expected to be due to the homogeneity of the PVP−chloroform mixture.

## AUTHOR INFORMATION

### Corresponding Author

*E-mail: naoki-ko@keyaki.cc.u-tokai.ac.jp.

## ACKNOWLEDGMENT

This work was supported in part by a Grant-in-Aid for Scientific Research (C)(22540420) and Research and Study Project of Tokai University Educational System General Research Organization.

## REFERENCES

(1) Stockhausen, M.; Abd-EL-Rehim, M. *Z. Naturforsch., A* **1994**, *49*, 1229.
(2) Murthy, S. S. N. *J. Phys. Chem. B* **2000**, *104*, 6955.
(3) Shinyashiki, N.; Sengwa, R. J.; Tsubotani, S.; Nakamura, H.; Sudo, S.; Yagihara, S. *J. Phys. Chem. A* **2006**, *110*, 4953.
(4) Tyagi, M.; Murthy, S. S. *Carbohydr. Res.* **2006**, *341*, 650.
(5) Shinyashiki, N.; Imoto, D.; Yagihara, S. *J. Phys. Chem. B* **2007**, *111*, 2181.
(6) Spanoudaki, A.; Shinyashiki, N.; Kyritsis, A.; Pissis, P. *AIP Conf. Proc.* **2008**, *982*, 125.
(7) Sudo, S.; Shimomura, M.; Kanari, K.; Shinyashiki, N.; Yagihara, S. *J. Chem. Phys.* **2006**, *124*, 044901.
(8) Cerveny, S.; Alegria, A.; Colmenero, J. *J. Chem. Phys.* **2008**, *128*, 044901.
(9) Cerveny, S.; Colmenero, J.; Alegría, Á. *Macromolecules* **2005**, *38*, 7056.
(10) Stockmayer, W. H. *Pure Appl. Chem.* **1967**, *15*, 539.
(11) Dachwitz, E. *Z. Naturforsch., A* **1990**, *45*, 126.
(12) Shinyashiki, N.; Asaka, N.; Mashimo, S.; Yagihara, S. *J. Chem. Phys.* **1990**, *93*, 760.
(13) Miura, N.; Shinyashiki, N.; Mashimo, S. *J. Chem. Phys.* **1992**, *97*, 8722.
(14) Shinyashiki, N.; Matsumura, Y.; Miura, N.; Yagihara, S.; Mashimo, S. *J. Phys. Chem.* **1994**, *98*, 13612.
(15) Shinyashiki, N.; Yagihara, S.; Arita, I.; Mashimo, S. *J. Phys. Chem. B* **1998**, *102*, 3249.
(16) Shinyashiki, N.; Yagihara, S. *J. Phys. Chem. B* **1999**, *103*, 4481.
(17) Kaatze, U. *Adv. Mol. Relax. Processes* **1975**, *7*, 71.
(18) Kaatze, U.; Gottmann, O.; Podbielski, R.; Pottel, R.; Terveer, U. *J. Phys. Chem.* **1978**, *82*, 112.
(19) Zaslavsky, B. Y.; Miheeva, L. M.; Rodnikova, M. N.; Spivak, G. V.; Harkin, V. S.; Mahmudov, A. U. *J. Chem. Soc., Faraday Trans. 1* **1989**, *85*, 2857.
(20) Jain, S. K.; Johari, G. P. *J. Phys. Chem.* **1988**, *92*, 5851.
(21) Asaka, N.; Shinyashiki, N.; Umehara, T.; Mashimo, S. *J. Chem. Phys.* **1990**, *93*, 8273.
(22) Chandra, R.; Xu, M.; Firman, P.; Eyring, E. M.; Petrucci, S. *J. Phys. Chem.* **1993**, *97*, 12127.
(23) Havriliak, S.; Negami, S. *Polymer* **1967**, *8*, 161.
(24) Cole, K. S.; Cole, R. H. *J. Chem. Phys.* **1941**, *9*, 341.
(25) Hill, N. E.; Vaughan, W. E.; Price, A. H.; Davies, M. *Dielectric Properties and Molecular Behaviour*; The Van Nostrand Series in Physical Chemistry; Van Nostrand Reinhold: London, 1969; pp 280−461.
(26) McCrum, N. G.; Read, B. E.; Williams, G. Theories of the Limiting Moduli and the Static Dielectric Constant. In *Anelastic and Dielectric Effects in Polymeric Solids*; John Wiley & Sons: London, 1967; pp 57−101.
(27) Schönhals, A. Molecular Dynamics in Polymer Model Systems In *A Broadband Dielectric Spectroscopy*; Kremer, F., Schönhals, A., Eds.; Springer: Berlin, 2003; pp 225−293.
(28) Yada, M.; Nakazawa, M.; Urakawa, O.; Morishima, Y.; Adachi, K. *Macromolecules* **2000**, *33*, 3368.
(29) Adachi, K.; Fujihara, I.; Ishida, Y. *J. Polym. Sci., Polym. Phys. Ed.* **1975**, *13*, 2155.
(30) Diaz-Calleja, R.; Riande, E. Calculation of Dipole Moments and Correlation Parameters. In *Dielectric Spectroscopy of Polymeric Materials: Fundamentals and Applications*; Runt, J. P., Fitzgerald, J. J., Eds.; American Chemical Society: Washington, DC, 1997; pp 139−173.
(31) Runt, J. P. Delectric Studies of Polymer Blends. In *Dielectric Spectroscopy of Polymeric Materials: Fundamentals and Applications*; Runt, J. P., Fitzgerald, J. J., Eds.; American Chemical Society: Washington, DC, 1997; pp 283−302.
(32) Mashimo, S. *Macromolecules* **1976**, *9*, 91.
(33) Ono, K.; Ueda, K.; Yamamoto, M. *Polym. J.* **1994**, *26*, 1345.
(34) Adolf, D. B.; Ediger, M. D.; Kitano, T.; Ito, K. *Macromolecules* **1992**, *25*, 867.
(35) Vogel, H. *Phys. Z.* **1921**, *22*, 645.
(36) Fulcher, G. S. *J. Am. Ceram. Soc.* **1923**, *8*, 339.
(37) Yoshizaki, K.; Urakawa, O.; Adachi, K. *Macromolecules* **2003**, *36*, 2349.
(38) Angell, C. A. *Science* **1995**, *267*, 1924.
(39) Jin, X.; Zhang, S.; Horvath, J. R.; Runt, J. *J. Phys. Chem. B* **2004**, *108*, 7681.
(40) Debye, P. *Polar Molecules*; Dover Publications: New York, 1929.
(41) Floudas, G.; Steffen, W.; Fischer, E. W.; Brown, W. *J. Chem. Phys.* **1993**, *99*, 695.
(42) Bawn, C. E.; Freeman, R. F. J.; Kamaliddin, A. R. *Trans. Faraday Soc.* **1950**, *46*, 677.
(43) Zhang; Painter, P. C.; Runt, J. *Macromolecules* **2002**, *35*, 9403.
(44) Böhmer, R.; Ngai, K. L.; Angell, C. A.; Plazek, D. J. *J. Chem. Phys.* **1993**, *99*, 4201.